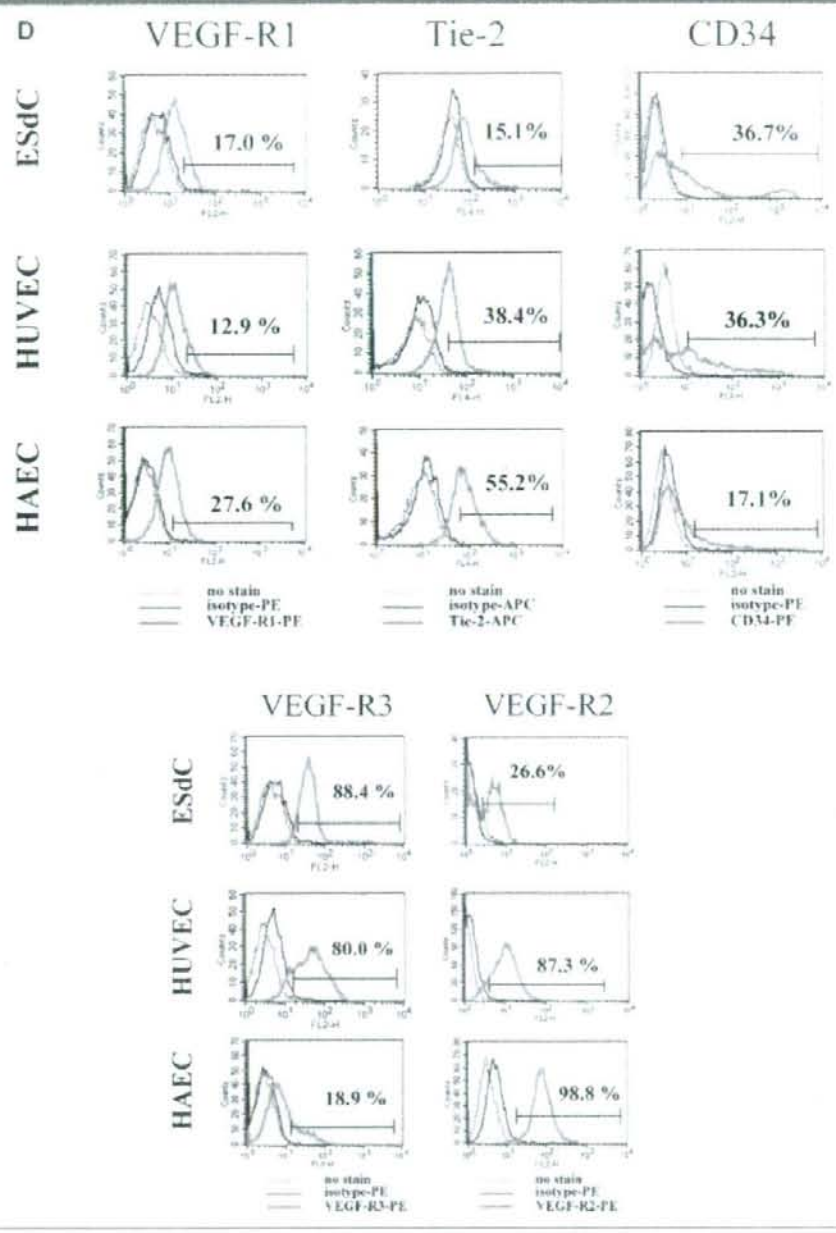

Fig. 3. ***(Continued)***

VE-cadherin-positive and VE-cadherin-negative populations showed quite similar spindle-shaped morphologies (but not polygonal shape) and were undistinguishable by microscopic observations (Figs. 5B and 6B). Indeed, our differentiated samples were negative for the expressions of smooth muscle actin (SMA)-α, a marker for smooth muscle cells, and PDGF receptor β, a marker for pericytes (Fig. 7A). As shown in Figure 7B,C, Nanog expression was not detected in ES-derived cells, excluding the possible existence of undifferentiated ES cells. Finally, genomic PCR studies excluded the contamination of MEFs, which were used only in the maintenance culture of undifferentiated cmES cells (Fig. 7D).

Thus, our novel method has enabled the highest efficiency vascular endothelial differentiation from primate ES cells,

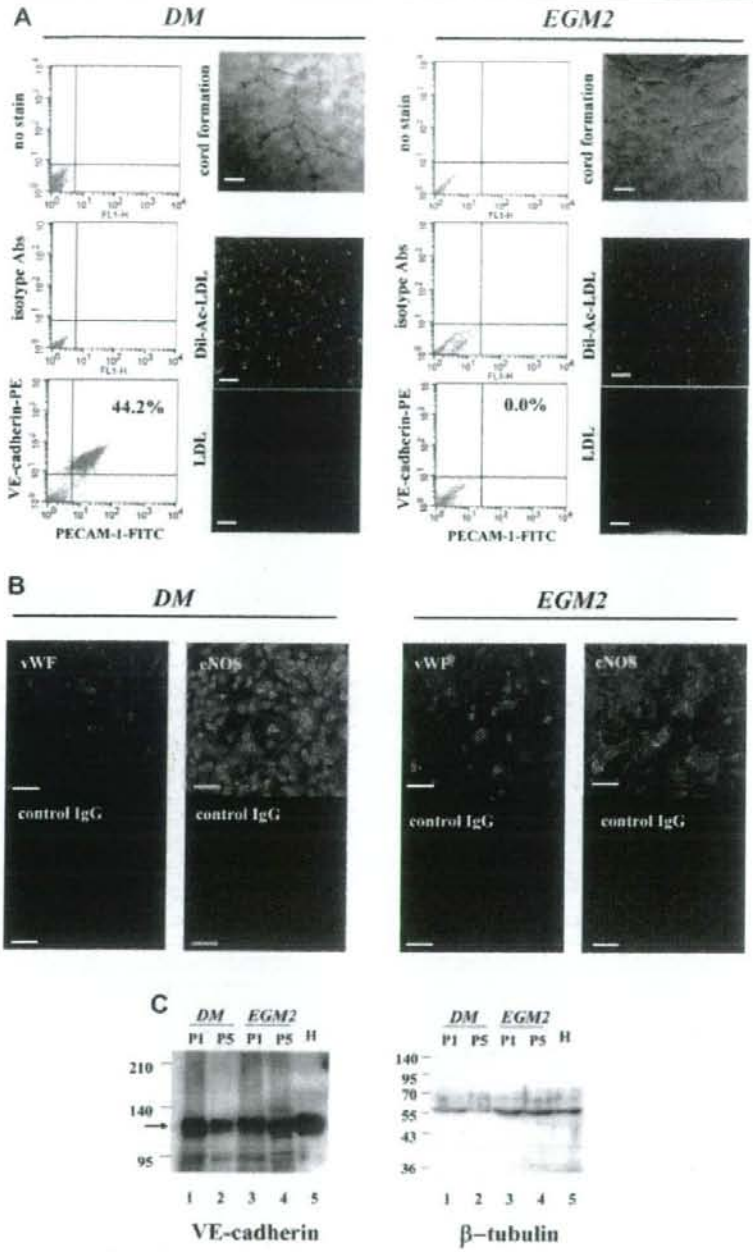

Fig. 4. Generation of atypical vascular endothelial cells by using commercially available culture medium. Differentiation procedure was performed either by using the differentiation medium supplemented with six cytokines (*DM*) or EGM®-2 BulletKit medium (*EGM2*). A: After two passages, flow cytometric analyses for cell surface VE-cadherin/PECAM-1 expressions (left parts), cord formation assays (right upper parts) and Ac-LDL uptaking assays (right lower parts) were performed in each culture condition (DM culture or EGM2 culture). The scale bar indicates 100 μm. B: After two passages, cells were fixed and stained by an anti-human vWF goat polyclonal antibody (red) and an anti-human eNOS rabbit polyclonal antibody (green). The scale bar indicates 50 μm. Similar results were obtained at passage number at least up to 7 (data not shown). C: At indicated numbers of passage, cells were collected and Western blotting was performed using an anti-human VE-cadherin rabbit polyclonal antibody. Arrows indicate the 130 kDa VE-cadherin protein (left part). For positive control, HUVEC lysate was used (lane 5, "H"). For internal control, β-tubulin expressions were determined (right part).

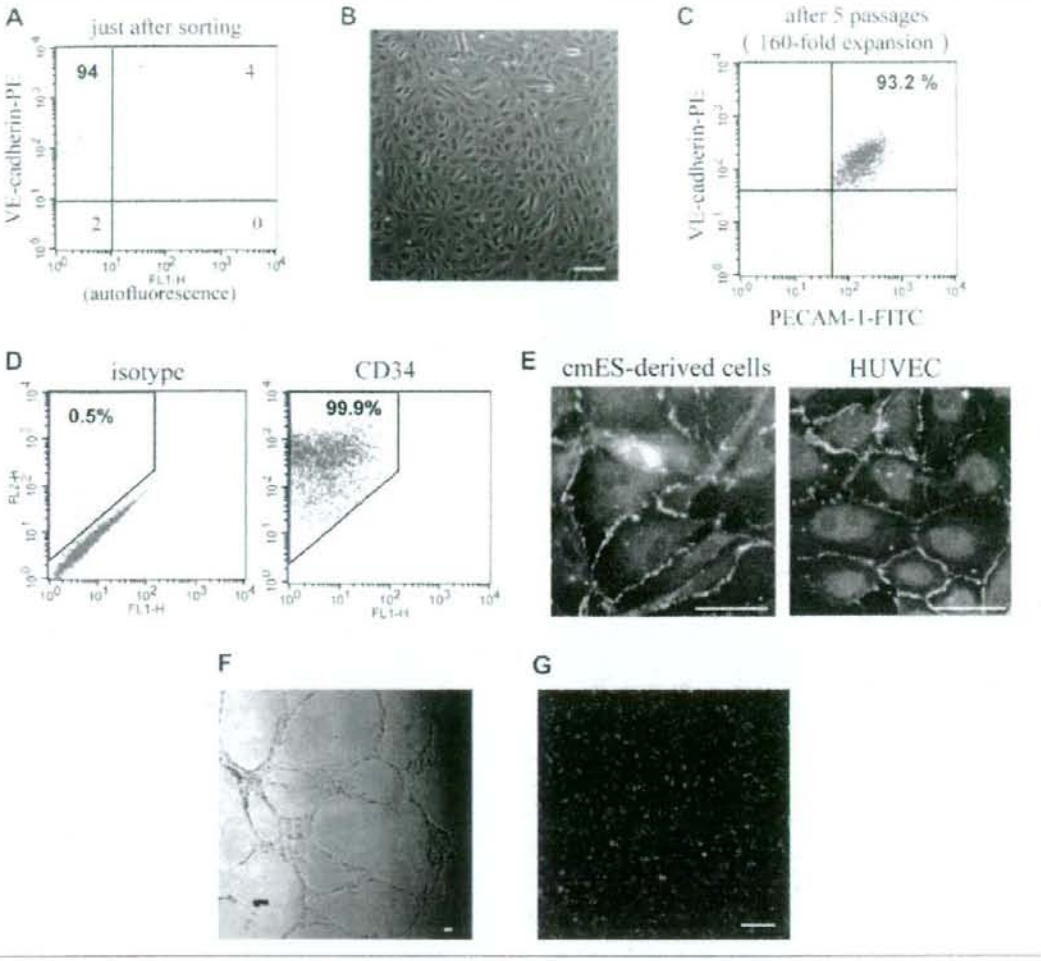

Fig. 5. Expansion and characterization of cell surface VE-cadherin-positive populations. Differentiation procedure was performed, and after the first passage, cell surface VE-cadherin-positive fraction was sorted by FACSAria™. A: The expression of VE-cadherin was determined just after sorting. B: After a few days culture, cell morphology was observed under an inverted phase contrast light microscope. The scale bar indicates 100 μm. C: After five passages, the cell surface expressions of VE-cadherin/PECAM-1 were re-studied by flow cytometry. D: The cell surface expression of CD34 was also studied by flow cytometry. E: Localization of VE-cadherin at intercellular junctions was confirmed by immunostaining using HUVEC as positive control. The scale bar indicates 50 μm. F,G: The functional analyses. Cord-forming activities (F) and Ac-LDL-uptaking capacities (G) were confirmed. The scale bar indicates 100 μm. H: Cell surface expressions of other endothelial markers (VEGF-R2, VEGF-R1, VEGF-R3, and Tie-2) were studied by flow cytometry.

providing pure production of vascular endothelial cells including VE-cadherin-negative "atypical" vascular endothelial cells.

The in vivo functions of ES-derived vascular endothelial cells

We next studied the in vivo functions of cmES-derived vascular endothelial cells by performing collagen sponge plug assays. Honeycomb collagen sponges were mixed with cmES-derived vascular endothelial cells (at passage 3) and transplanted intraperitoneally into SCID mice. After 35 days, FITC-dextran was injected from tail vein and then plugs were excited and histologically examined. As shown in Figure 8A, multiple FITC-dextran-filled lumens were detected in the collagen plugs, indicating the presence of neovascularization connected with systematic circulation within the plugs. Histological observations further confirmed the presence of neovascularization, which was filled with erythrocytes (Fig. 8B). The cells that lined the neovascular lumens as well as the cells remaining within the honeycomb plugs were all stained by both an anti-human HLA-A, B, C antibody (Fig. 8C, left middle part), which distinguishes primate cells from murine cells (Kaufman et al., 2004), and by an anti-human PECAM-1 antibody (Fig. 8C, right middle parts) which shows their endothelial nature. Finally, these vascular structures with human (primate)

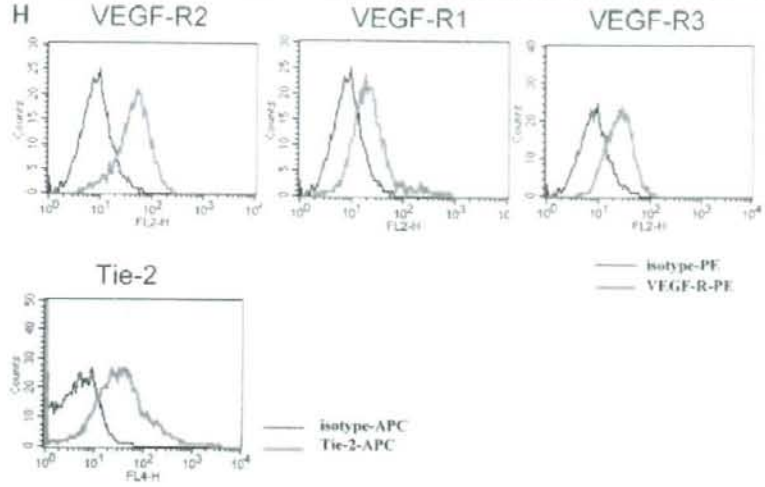

Fig. 5. (*Continued*)

HLA and PECAM-1 were again shown to be connected with systematic circulation (Fig. 8C, lower left and right parts).

Thus, the cmES-derived vascular endothelial cells produced by our method are functional in vivo.

Evaluation of the roles of each medium component for effective differentiation

Finally, we re-evaluated the requirement of each component of our differentiation medium for vascular endothelial differentiation of cmES cells. First we studied the necessity of each cytokine for the generation of spheres, sac-like structures and cell surface VE-cadherin/PECAM-1-positive cells by checking the effects of depletion of each one cytokine from differentiation medium.

Depletion of IL-3 or IL-6 deteriorated the quality of spheres: the spheres often failed to proliferate during subsequent adherent culture (data not shown). In regard to the other four cytokines (BMP-4, SCF, Flt3-L, and VEGF), depletion of BMP-4 resulted in the formation of sac-like structures with poor hematopoiesis (Fig. 9A). On the other hand, depletion of SCF, Flt3-L and VEGF did not affect the formation of sac-like structures (Fig. 9A).

When estimated by the performance for the induction of cell surface VE-cadherin/PECAM-1-positive cells, all of the four cytokines BMP-4, SCF, Flt3-L and VEGF were found to play important roles in differentiation. Depletion of BMP-4, SCF, or Flt3-L deteriorated the performance levels in producing cell surface VE-cadherin/PECAM-1-positive cells (Fig. 9C,D). Although in some cases, depletion of each cytokine did not dramatically reduce the percentages of cell surface VE-cadherin/PECAM-1-positive cells (Fig. 9C), it did abolish the generation of cell surface VE-cadherin/PECAM-1-positive cells in other cases (Fig. 9B). Approximately estimated, one out of three experiments, we failed in generation of cell surface VE-cadherin/PECAM-1-double-positive cells when BMP-4, SCF, or Flt3-L was depleted from the medium. Depletion of VEGF reproducibly reduced the percentages of cell surface VE-cadherin/PECAM-1-positive cells (Fig. 9B,C). In contrast, replacement of IMDM by RPMI 1640 medium did not affect the all processes of differentiation (Fig. 9A–C). On the other hand, no sac-like structures were generated by EGM®-2 BulletKit cultures even when supplemented with six cytokines or six cytokines plus 10% FBS (Fig. 9A). In addition, percentages of cell surface VE-cadherin/PECAM-1-positive cells were considerably low (Fig. 9B–C), a finding almost identical to EGM®-2 BulletKit culture without six cytokines (Fig. 4A, EGM part).

Thus, it was concluded that (1) IL-3 and IL-6 contribute to the improvement of the quality of spheres, (2) BMP-4 is essential for a sac-dependent hematopoiesis, (3) VEGF is critical for the production of cell surface VE-cadherin/PECAM-1-positive cells, (4) BMP-4, SCF and Flt3-L contribute to the stable induction of cell surface VE-cadherin/PECAM-1-positive cells, and (5) Differentiation medium can be prepared by using RPMI 1640 in place of IMDM, but not by using EGM®-2 BulletKit, for the production of a sac-like structure and cell surface VE-cadherin/PECAM-1-positive cells.

Discussion

In this article, we reported a method for high efficiency differentiation of vascular endothelial cells from feeder-free primate ES cells. cmES-derived vascular endothelial cells are subculturable and freeze–thaw-tolerable. An additional merit of our system is its feasibility: it does not require a process to sort the progenitor populations such as VEGF-R2-positive (Sone et al., 2003, 2007) or CD34-positive (Wang et al., 2007) fractions. To our knowledge, this is the highest efficiency system for the production of vascular endothelial cells. Indeed, our system provides almost two pure populations: the cell surface VE-cadherin/PECAM-1-positive "canonical" vascular endothelial cells and cell surface VE-cadherin/PECAM-1-negative "atypical" vascular endothelial cells. Co-existence of pericytes was excluded. Contamination of immature Nanog-expressing ES cells was also excluded. Eventually, no tumor formation was observed after transplanting the cmES-derived vascular endothelial cells into SCID mice (data not shown), encouraging a safe application of

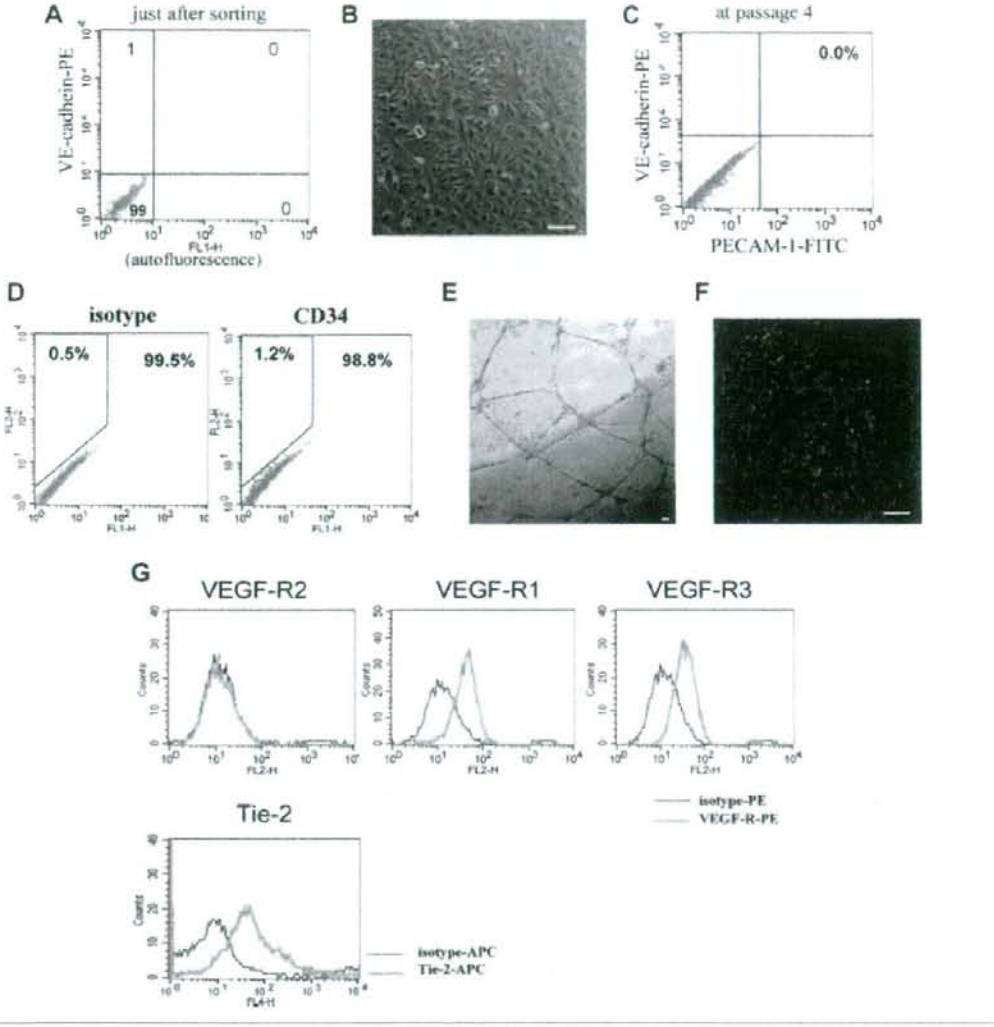

Fig. 6. Expansion and characterization of cell surface VE-cadherin-negative populations. Differentiation procedure was performed, and after the first passage, cell surface VE-cadherin-negative fraction was sorted by FACSAria™. A: The expression of VE-cadherin was determined just after sorting. B: After a few days culture, cell morphology was observed under an inverted phase contrast light microscope. The scale bar indicates 100 μm. C: After four passages, the cell surface expressions of VE-cadherin/PECAM-1 were re-studied by flow cytometry. D: The cell surface expression of CD34 was also studied by flow cytometry. E,F: The functional analyses. Cord-forming activities (E) and Ac-LDL-uptaking capacities (F) were confirmed. The scale bar indicates 100 μm. G: Cell surface expressions of other endothelial markers (VEGF-R2, VEGF-R1, VEGF-R3, and Tie-2) were studied by flow cytometry. H: VE-cadherin expression was determined by immunostaining studies. The cells were stained by an anti-VE-cadherin antibody (upper) or isotype control antibody (lower). The right parts indicate the phase contrast microscopy. The scale bar indicates 50 μm. I: Western blotting of VE-cadherin (left) and β-tubulin (right) of the cell surface VE-cadherin-negative population (lane 1) and the total population before sorting (lane 2). The expression of 130-kDa VE-cadherin band (indicated by arrow) was detected even in the cell surface VE-cadherin-negative population, indicating the intracellular localization of VE-cadherin. J: RT-PCR studies for VE-cadherin (upper) and β-actin (lower) were shown. The templates used were as follows: lane 1; cDNA of the cell surface VE-cadherin-negative population, lane 2; cDNA of total populations before sorting, lane 3; cDNA of HUVEC, lane 4; water, lane 5; cDNA of hematopoietic HL-60 cells. K,L: Immunostaining studies and flow cytometric analyses of hematopoietic and monocyte/macrophage markers. K: Cells were stained by an isotype control antibody (left) or an anti-CD68 antibody (right). Lower parts indicate the photographs with Normarsky differentiated interference contrast. The scale bar indicates 100 μm. L: Cell surface expressions of CD14 (upper, a bold green line), CD18 (middle, a bold green line), CD11b (lower, a bold green line), and CD45 (lower, a bold pink line) were studied. Thin black lines indicate the data of non-staining samples and bold black lines indicate the data of isotype control antibody-stained samples.

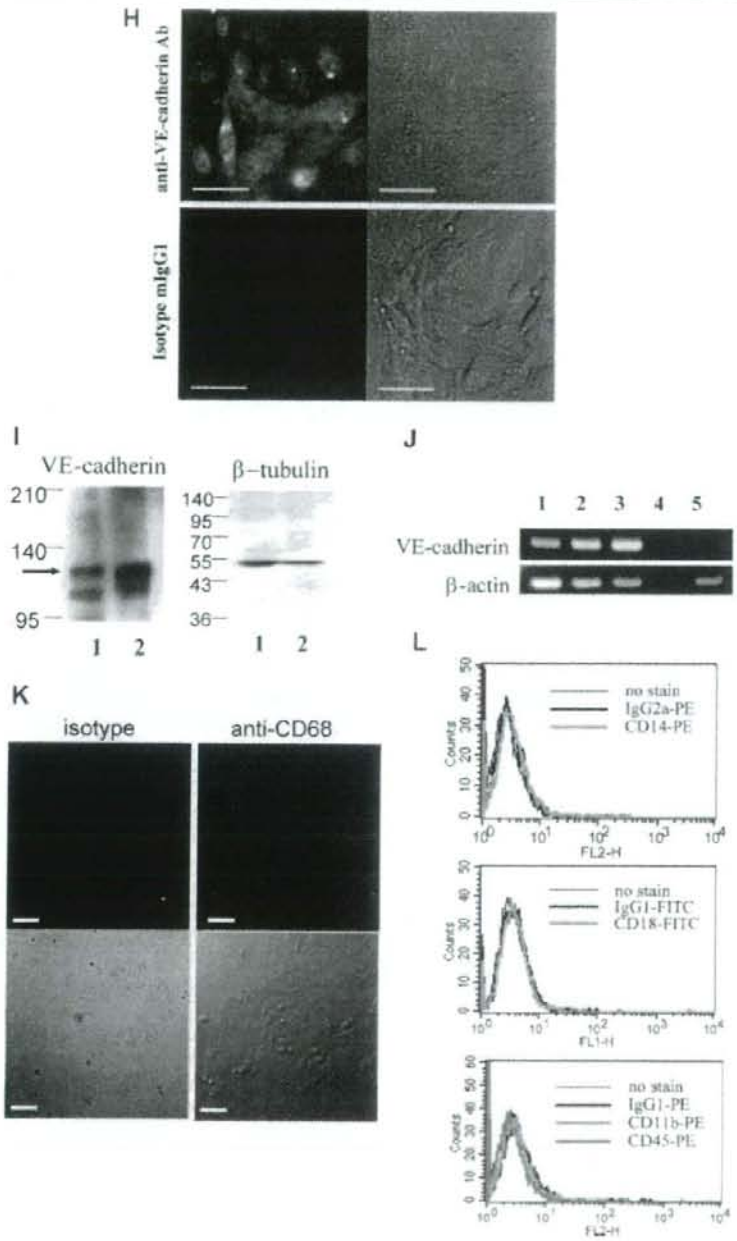

Fig. 6. ***(Continued)***

human ES-derived endothelial cells to clinical purposes in future.

Technically, our differentiation method has two unique points. One is the two-step protocol, where a sphere formation is followed by adherent culture. Although a short sphere-forming process was performed in our system, we could obtain clear microscopic fields owing to the subsequent adherent culture step, during which cells proliferated and

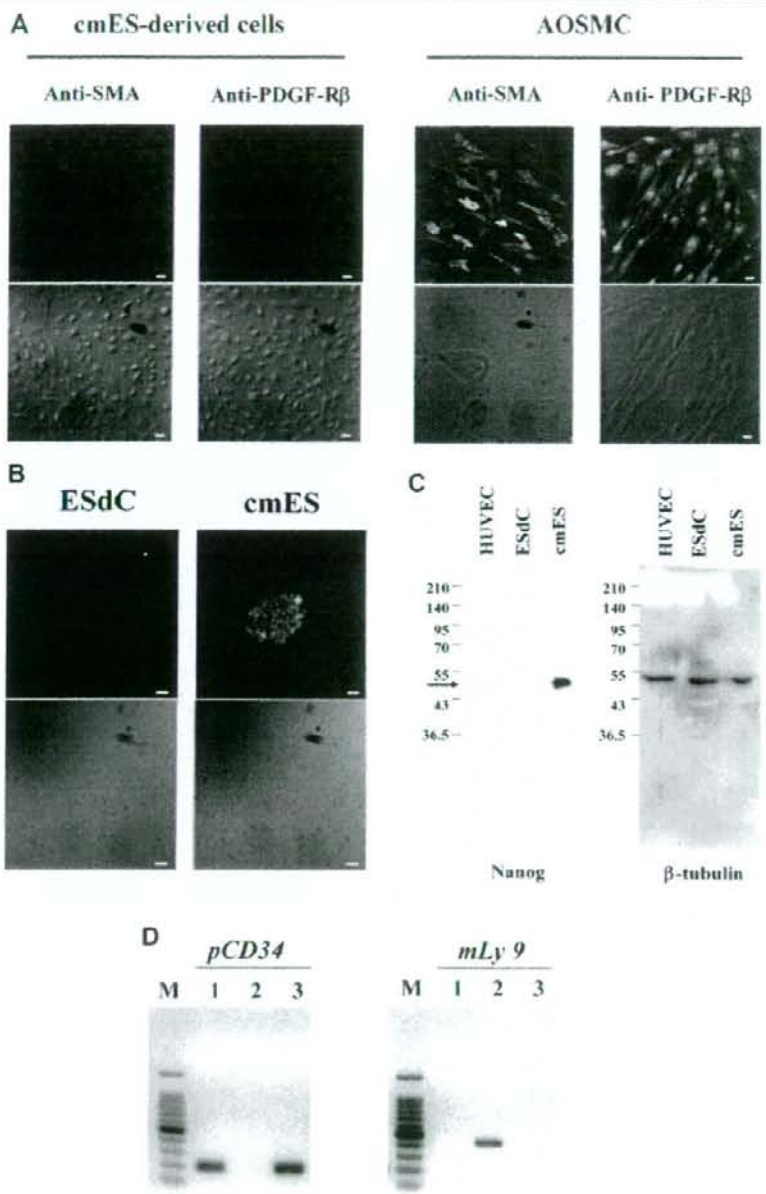

Fig. 7. Possible existence or contamination of pericytes, undifferentiated ES cells and MEFs was investigated. A: Possible existence of pericytes in cmES-derived cells was studied based upon smooth muscle specific markers (SMA and PDGF-Rβ). cmES-derived cells (left parts) were fixed and stained by anti-SMA antibody or anti-PDGF-Rβ antibody as indicated. As a positive control, human aortic smooth muscle cells (AOSMC) were used. The scale bar indicates 20 μm. B,C: Possible existence or contamination of undifferentiated cmES cells in cmES-derived cells (ESdC) was studied based upon undifferentiated ES cell marker, Nanog. The ESdC or undifferentiated cmES cells were fixed and stained by anti-human Nanog antibody (B) or were lysed and subjected to Western blotting using anti-Nanog antibody (C, left). An arrow indicates the expression of 50-kDa Nanog protein. For internal control, β-tubulin expression was examined (C, right). The scale bar indicates 100 μm. D: Possible contamination of MEFs in cmES-derived cells was studied using primate and murine specific markers. Genomic DNA was extracted from HUVECs (lane 1), MEFs (lane 2), and cmES-derived cells (lane 3). PCR was performed using the primers for primate CD34 genomic fragment (left column; *pCD34*) or those for murine ly 9.2 genomic fragment (right column; *mLy9*).

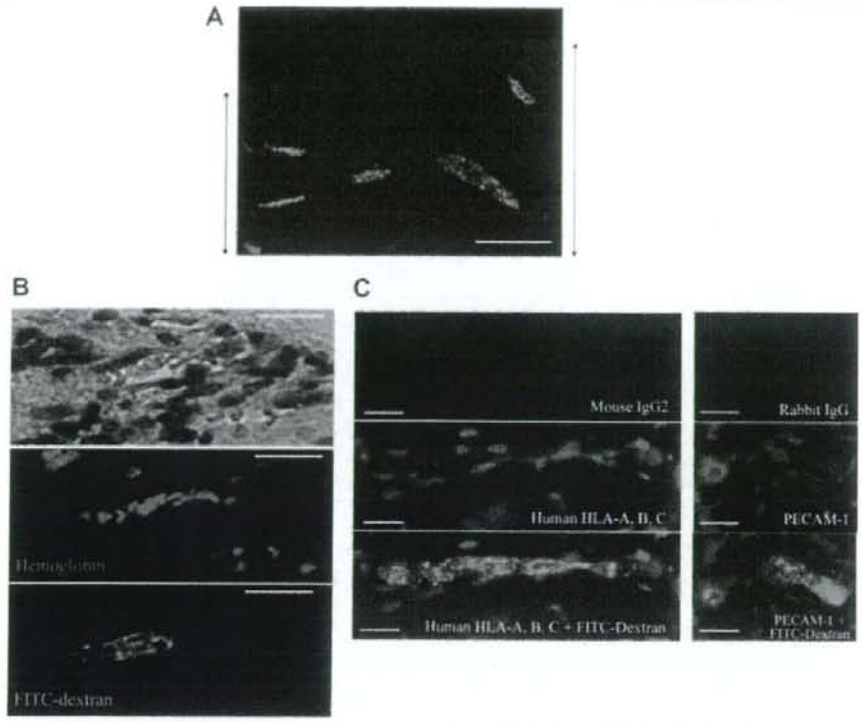

Fig. 8. The in vivo functions of cmES-derived cells. cmES-derived cells were cultured in honeycomb collagen sponges for 2 days in vitro and were then transplanted intraperitoneally into SCID mice. At day 35, FITC-dextran was injected into the transplanted mouse from a tail vein. Then collagen plugs were taken out, fixed, embedded and sliced as described in Materials and Methods Section. A: Fluorescence microscopic observations of FITC-dextran in sliced honeycomb collagen sponges. The scale bar indicates 100 μm. B: The microscopic observation of hematoxylin-eosin-stained samples (upper) and fluorescence microscopic observations of autofluorescence of hemoglobins (middle) and FITC-dextran (lower). Scale bars indicate 20 μm. C: Immunostaining studies were performed using indicated antibodies. The positive staining by anti-human PECAM-1 and anti-human HLA-A, B, C antibodies indicates the recruitment of cmES-derived cells into the neovascularity. Scale bars indicate 20 μm.

spread out almost like a monolayer culture. Hence, we could identify a unique construction, a sac-like structure surrounded by cobblestone cells, as the parental organization for vascular endothelial cells. Recently, the existence of this "sac-like" structure was independently reported (Ma et al., 2007), where human ES cells were co-cultured with murine OP9 stromal cells. Interestingly, they reported that the sac-like structures emerged with the same time course (around 12 days after co-culture) as our system. Because we applied the feeder-free culture method, we could detect the presence of surrounding cobblestone cells, which might possibly be merged with OP9 cells in their system. By immunostaining studies, we further noticed that both sac wall cells and surrounding cobblestone cells expressed VE-cadherin at intercellular junctions (Fig. 1D).

Another point of our success may reside in the formula of our differentiation medium. In contrast to previous reports, where a commercially available vascular endothelial cell-specific medium of EGM®-2 MV BulletKit was used (Kaufman et al., 2004; Wang et al., 2007), we prepared the differentiation medium by modifying the culture medium optimized to hematopoietic differentiation (Li et al., 2001). As our original aim was to produce hematopoietic stem cells, we deleted GM-CSF, G-CSF, erythropoietin and hydrocortisone, which rather work in later and mature phases of hematopoiesis, from the formula by Li et al. (2001). After we had established our method for high efficiency differentiation of vascular endothelial cells, we re-evaluated the necessity of each cytokine and found that the differentiation medium was indeed optimal. Among six cytokines, the role of VEGF is very clear: it is required for production of cell surface VE-cadherin/PECAM-1-positive population. Other cytokines including BMP-4, IL-3, IL-6, SCF and FLt3-L are required for the better performance of differentiation. Literally, BMP-4 is required for the generation of Scl/Tal-1-positive hemangioblast cells from murine ES cells (Park et al., 2004). IL-3 and SCF are reportedly effective in inducing vascular endothelial cells from murine hematopoietic cells (Yamada and Takakura, 2006). Recently, it was reported that IL-6 promotes choroidal neovascularization (Izumi-Nagai et al., 2007). Thus, it seems that every hematopoietic cytokine is involved in specific phase of vascular endothelial differentiation although its precise roles are not yet determined. Our usage of multiple hematopoietic cytokines possibly contributed to the prevention of emergence and/or proliferation of pericytes, which are often generated with vascular endothelial cells during

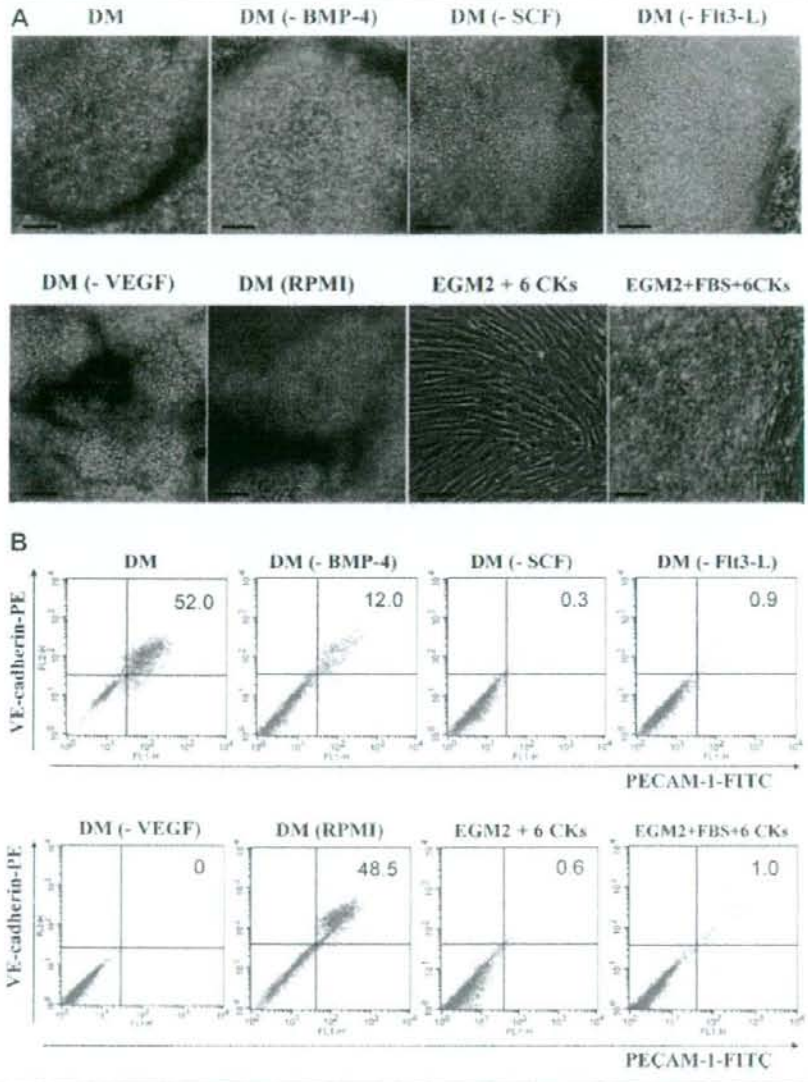

Fig. 9. The roles of medium components for vascular endothelial differentiation. The differentiation procedure was performed by depleting BMP-4 (DM(-BMP-4)), SCF (DM(-SCF)), Flt3-L (DM(-Flt3-L)) or VEGF (DM(-VEGF)) from the differentiation medium (DM), using differentiation medium prepared by using RPMI 1640 in place of IMDM (DM(RPMI)), using EGM®-2 BulletKit medium supplemented with all six cytokines (EGM2 + 6CKs), or using EGM®-2 BulletKit medium supplemented with 10% FBS and all six cytokines (EGM2 + FBS + 6CKs). A: The phase contrast micrographs. Note that BMP-4 depletion resulted in deficient production of inner round cells. Scale bars indicate 50 μm. B,C: Flow cytometric analyses for cell surface VE-cadherin/PECAM-1 expressions. From a number of experiments, we obtained two patterns of results shown in (B) and (C) with 1:2 frequencies (data not shown).

differentiation of ES cells and inhibit the expansion of vascular endothelial cells. Of course, further studies are required for the total understanding of the hematopoietic/endothelial differentiation mechanism from primate ES cells.

In this report, we termed the cells that are cell surface VE-cadherin/PECAM-1-negative but otherwise are equivalent to vascular endothelial cells as "atypical vascular endothelial cells." These cells seem to be frequently produced during primate ES differentiation (Kaufman et al., 2004). Whether the existence of atypical vascular endothelial cells is restricted to in vitro differentiation system or there are in vivo counterparts is a matter of great interest. It is known that fractions of adult human peripheral monocytes can give rise to endothelial-like cells. For example, monocyte-derived immature dendritic cells

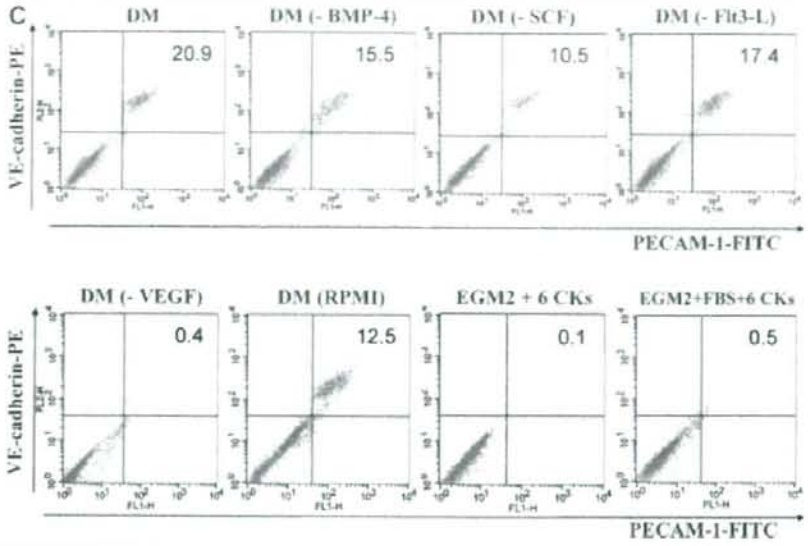

Fig. 9. ***(Continued)***

(Fernandez Pujol et al., 2001) and monocyte-derived multi-potential cells (Kuwana et al., 2006) can produce functionally maturated vascular endothelial cells. Our cmES-derived cells are, however, negative for monocyte markers including CD68, CD14 and CD11b (Fig. 6K,L). As for now, it is not yet determined whether they belong to a novel endothelial population or they represent a transient state during which monocytic precursors are differentiating into vascular endothelial cells. Future investigation will be required for the evaluation of atypical vascular endothelial cells in vivo.

The ES-derived vascular endothelial cells generated by our method are subculturable up to eight passages, after which they undergo senescence (unpublished observation). Aging cells show enlarged morphologies and become positive in senescence-associated β-galactosidase activity assays along with p38 activation and p16 induction. The reason for this stress-induced senescence remains elusive. Although the senescence induction in ES-derived vascular endothelial cells may put certain restrictions on their usage, it may exclude the possible tumorigenesis via unlimited proliferation after transplantation. Moreover, our ES-derived vascular endothelial cells can be used for researches on stress-induced senescence, providing tools for investigations on mechanisms of vascular complication development in lifestyle-related stress-associated diseases such as diabetes mellitus (Yokoi et al., 2006) hypertension (Kobayashi et al., 2006) and atherosclerosis (Minamino et al., 2002).

Our differentiation method is applicable to human ES cells: the high efficiency vascular endothelial differentiation (~70%) with proper in vitro and in vivo functions has been achieved by using human ES cells and the same differentiation protocol (M. Nakahara, in preparation). Of course, human ES cells cannot be directly applied to regenerative medicine because of an immunological hurdle. However, when the hurdle will be overcome via a nuclear transfer technique (Byrne et al., 2007) or when iPS cells (Takahashi et al., 2007; Yu et al., 2007) will be improved for safety application to clinical usages, our method will provide the most effective tool for regenerative medicine targeted to vascular endothelial disorders.

Literature Cited

Byrne JA, Pedersen DA, Clepper LL, Nelson M, Sanger WG, Gokhale S, Wolf DP, Mitalipov SM. 2007. Producing primate embryonic stem cells by somatic cell nuclear transfer. Nature 450:497–502.

Fernandez Pujol B, Lucibello FC, Zuzarte M, Lütjens P, Müller R, Havemann K. 2001. Dendritic cells derived from peripheral monocytes express endothelial markers and in the presence of angiogenic growth factors differentiate into endothelial-like cells. Eur J Cell Biol 80:99–110.

Hirashima M, Kataoka H, Nishikawa S, Matsuyoshi N, Nishikawa S. 1999. Maturation of embryonic stem cells into endothelial cells in an in vitro model of vasculogenesis. Blood 93:1253–1263.

Izumi-Nagai K, Nagai N, Ozawa Y, Mihara M, Ohsugi Y, Kurihara T, Koto T, Satofuka S, Inoue M, Tsubota K, Okano H, Oike Y, Ishida S. 2007. Interleukin-6 receptor-mediated activation of signal transducer and activator of transcription-3 (STAT3) promotes choroidal neovascularization. Am J Pathol 170:2149–2158.

Kaufman DS, Lewis RL, Hanson ET, Auerbach R, Plendl J, Thomson JA. 2004. Functional endothelial cells derived from rhesus monkey embryonic stem cells. Blood 103:1325–1332.

Kobayashi K, Imanishi T, Akasaka T. 2006. Endothelial progenitor cell differentiation and senescence in an angiotensin II-infusion rat model. Hypertens Res 29:449–455.

Kuwana M, Okazaki Y, Kodama H, Satoh T, Kawakami Y, Ikeda Y. 2006. Endothelial differentiation potential of human monocyte-derived multipotential cells. Stem Cells 24:2733–2743.

Levenberg S, Golub JS, Amit M, Itskovitz-Eldor J, Langer R. 2002. Endothelial cells derived from human embryonic stem cells. Proc Natl Acad Sci USA 99:4391–4396.

Li F, Lu S, Vida L, Thomson JA, Honig GR. 2001. Bone morphogenetic protein 4 induces efficient hematopoietic differentiation of rhesus monkey embryonic stem cells in vitro. Blood 15:335–432.

Ma F, Wang D, Hanada S, Ebihara Y, Kawasaki H, Zaike Y, Heike T, Nakahata T, Tsuji K. 2007. Novel method for efficient production of multipotential hematopoietic progenitors from human embryonic stem cells. Int J Hematol 85:371–379.

Minamino T, Miyauchi H, Yoshida T, Ishida Y, Yoshida H, Komuro I. 2002. Endothelial cell senescence in human atherosclerosis: Role of telomere in endothelial dysfunction. Circulation 105:1541–1544.

Park C, Afrikanova I, Chung YS, Zhang WJ, Arentson E, Fong Gh G, Rosendahl A, Choi K. 2004. A hierarchical order of factors in the generation of FLK1- and SCL-expressing hematopoietic and endothelial progenitors from embryonic stem cells. Development 131:2749–2762.

Saeki K, Hong Z, Nakatsu M, Yoshimori T, Kabeya Y, Yamamoto A, Kaburagi Y, Yuo A. 2003. Insulin-dependent signaling regulates azurophil granule-selective macroautophagy in human myeloblastic cells. J Leukoc Biol 74:1108–1116.

Sato N, Meijer L, Skaltsounis L, Greengard P, Brivanlou AH. 2004. Maintenance of pluripotency in human and mouse embryonic stem cells through activation of Wnt signaling by a pharmacological GSK-3-specific inhibitor. Nat Med 10:55–63.

Sone M, Itoh H, Yamashita J, Yurugi-Kobayashi T, Suzuki Y, Kondo Y, Nonoguchi A, Sawada N, Yamahara K, Miyashita K, Park K, Shibuya M, Nito S, Nishikawa S, Nakao K. 2003.

Different differentiation kinetics of vascular progenitor cells in primate and mouse embryonic stem cells. Circulation 107:2085–2088.
Sone M, Itoh H, Yamahara K, Yamashita JK, Yurugi-Kobayashi T, Nonoguchi A, Suzuki Y, Chao TH, Sawada N, Fukunaga Y, Miyashita K, Park K, Oyamada N, Sawada N, Taura D, Tamura N, Kondo Y, Nito S, Suemori H, Nakatsuji N, Nishikawa S, Nakao K. 2007. Pathway for differentiation of human embryonic stem cells to vascular cell components and their potential for vascular regeneration. Arterioscler Thromb Vasc Biol 27:2127–2134.
Suemori H, Tada T, Torii R, Hosoi Y, Kobayashi K, Imahie H, Kondo Y, Iritani A, Nakatsuji N. 2001. Establishment of embryonic stem cell lines from cynomolgus monkey blastocysts produced by IVF or ICSI. Dev Dyn 222:273–279.
Takagi Y, Takahashi J, Saiki H, Morizane A, Hayashi T, Kishi Y, Fukuda H, Okamoto Y, Koyanagi M, Ideguchi M, Hayashi H, Imazato T, Kawasaki H, Suemori H, Omachi S, Iida H, Itoh N, Nakatsuji N, Sasai Y, Hashimoto N. 2005. Dopaminergic neurons generated from monkey embryonic stem cells function in a Parkinson primate model. J Clin Invest 115: 102–109.
Takahashi K, Tanabe K, Ohnuki M, Narita M, Ichisaka T, Tomoda K, Yamanaka S. 2007. Induction of pluripotent stem cells from adult human fibroblasts by defined factors. Cell 131:861–872.
Vodyanik MA, Bork JA, Thomson JA, Slukvin II. 2005. Human embryonic stem cell-derived CD34+ cells: Efficient production in the coculture with OP9 stromal cells and analysis of lymphohematopoietic potential. Blood 105:617–626.
Wang ZZ, Au P, Chen T, Shao Y, Daheron LM, Bai H, Arzigian M, Fukumura D, Jain RK, Scadden DT. 2007. Endothelial cells derived from human embryonic stem cells form durable blood vessels in vivo. Nat Biotechnol 25:317–318.
Yamada Y, Takakura N. 2006. Physiological pathway of differentiation of hematopoietic stem cell population into mural cells. J Exp Med 203:1055–1065.
Yamashita J, Itoh H, Hirashima M, Ogawa M, Nishikawa S, Yurugi T, Naito M, Nakao K, Nishikawa S. 2000. Flk1-positive cells derived from embryonic stem cells serve as vascular progenitors. Nature 408:92–96.
Yokoi T, Fukuo K, Yasuda O, Hotta M, Miyazaki J, Takemura Y, Kawamoto H, Ichijo H, Ogihara T. 2006. Apoptosis signal-regulating kinase 1 mediates cellular senescence induced by high glucose in endothelial cells. Diabetes 55:1660–1665.
Yu J, Vodyanik MA, Smuga-Otto K, Antosiewicz-Bourget J, Frane JL, Tian S, Nie J, Jonsdottir GA, Ruotti V, Stewart R, Slukvin II, Thomson JA. 2007. Induced pluripotent stem cell lines derived from human somatic cells. Science 318:1917–1920.

STEM CELLS AND DEVELOPMENT 17:641–652 (2008)

DOI: 10.1089/scd.2008.0088

Inhibition of Mouse GPM6A Expression Leads to Decreased Differentiation of Neurons Derived from Mouse Embryonic Stem Cells

Hideo Michibata,[1,2] Tsuyoshi Okuno,[1] Nae Konishi,[1] Koji Wakimoto,[1] Kiyoshi Kyono,[1] Kan Aoki,[1] Yasushi Kondo,[1] Kazuyuki Takata,[2] Yoshihisa Kitamura,[2] and Takashi Taniguchi[2]

Glycoprotein M6A (GPM6A) is known as a transmembrane protein and an abundant cell surface protein on neurons in the central nervous system (CNS). However, the function of GPM6A is still unknown in the differentiation of neurons derived from embryonic stem (ES) cells. To investigate the function of GPM6A, we generated knockdown mouse ES cell lines (D3m-shM6A) using a short hairpin RNA (shRNA) expression vector driven by the U6 small nuclear RNA promoter, which can significantly suppress the expression of mouse GPM6A mRNA. Real-time polymerase chain reaction (real-time PCR) and immunocytochemical analysis showed that expression of shRNA against GPM6A markedly reduced the expression of neuroectodermal-associated genes (*OTX1, Lmx1b, En1, Pax2, Pax5, Sox1, Sox2,* and *Wnt1*), and also the number of neural stem cells (NSC) derived from D3m-shM6A cells compared to control vector–transfected mouse ES cells (D3m-Mock). Moreover, our results show a decrease in both the number of neuronal markers and the number of differentiating neuronal cells (cholinergic, catecholaminergic, and GABAergic neurons) from NSC in D3m-shM6A cells. Hence, our findings suggest that expression level of GPM6A is directly or indirectly associated with the differentiation of neurons derived from undifferentiated ES cells.

Introduction

EMBRYONIC STEM (ES) cells are continuously growing cells derived from the inner cell mass of preimplantation stage embryos [1,2], and can be cultured in an undifferentiated state in vitro for extended periods of time. ES cells can give rise in vitro to various cell types, including neurons, pancreatic cells, and hematopoietic cells [3–7]. The rate of ES cell differentiation is affected by induction or inhibition of certain gene expressions. Neurons are generated from ES cells through neural stem cells (NSC) in embryoid bodies (EB) [5,6]. Recently, Nakayama et al. [7] have developed a simple method to efficiently produce NSC from undifferentiated ES cells under free-floating conditions in astrocyte-conditioned medium (ACM) without formation of EB.

Glycoprotein M6A (GPM6A), which shows high homology with the proteolipid protein (PLP/DM20), is a transmembrane protein and an abundant cell surface protein on neurons in the central nervous system (CNS) [8]. Studies of PLP/DM20 family expression show that GPM6A is present in neurons, GPM6B in both neurons and glia, and PLP/DM20 in oligodendrocytes [9]. It is reported that in the hippocampus chronic psychosocial stress decreases the expression level of GPM6A and that chronic administration of antidepressants prevents this downregulation [10,11]. Mukobata et al. [12] reported that Ca^{2+} influx is increased by treatment with nerve growth factor (NGF) in rat pheochromocytoma PC12 cells with overexpression of GPM6A and that anti-GPM6A antibody suppresses both NGF-triggered Ca^{2+} influx and neuronal differentiation. A recent study has shown that the overexpression of GPM6A induces filopodium formation in neuronal and nonneuronal cell lines, and that GPM6A knockdown decreases filopodium density and reduces synaptic density in hippocampal neurons [13]. However, it is unclear whether GPM6A is related to the differentiation of neurons from undifferentiated ES cells.

[1]Advanced Medical Research Laboratory, Mitsubishi Tanabe Pharma Corporation, Yodogawa-ku, Osaka, Japan.
[2]Department of Neurobiology, Kyoto Pharmaceutical University, Misasagi, Yamashina-ku, Kyoto, Japan.

To investigate the function of GPM6A in neural differentiation, we have generated knockdown mouse ES cell lines expressing short hairpin RNA (shRNA) against GPM6A. In the present study, we show that RNA interference with GPM6A function causes a reduction of mRNA levels in neuroectodermal markers (OTX1: transcription factor required for the maintenance and regionalization of the forebrain and midbrain during development [14,15]; Lmx1b: transcription factor required for the limb bud development [16,17]; En1, Pax2, Pax5, and Wnt1: transcription factors involved in mid/hindbrain development [18–22]; Sox1 and Sox2: transcription factors expressed by developing nervous system [23,24]) and decreases neural differentiation both from undifferentiated mouse ES cells to NSC and from NSC to neuronal cells.

Materials and Methods

Cell culture

COS-7 cells were purchased from Dainippon Sumitomo Pharma Co. Ltd. (Osaka, Japan) and cultured in Dulbecco's modified Eagle's medium (DMEM) (Invitrogen Corp., Carlsbad, CA, USA), supplemented with 10% fetal calf serum (FCS), 100 U/ml penicillin (Sigma Chemical Co. Ltd., St. Louis, MO, USA), 0.1 mg/ml streptomycin (Sigma), and 2 mM L-glutamine (Sigma) at 37°C in 5% CO_2.

D3 mouse ES cell line was purchased from American Type Culture Collection (Manassas, VA, USA). ES cells were maintained on mitomycin C (Kyowa Hakko Kogyo Co. Ltd., Shizuoka, Japan)-treated mouse embryonic fibroblasts in DMEM/F12 (Sigma) supplemented with 13% FCS, 100 U/ml penicillin, 0.1 mg/ml streptomycin, 2 mM L-glutamine, 1 mM sodium pyruvate (Sigma), 0.1% sodium bicarbonate (Sigma), 0.1 mM 2-mercaptoethanol (Sigma), and 1,000 U/ml ESGRO (Chemicon International, Inc., Temecula, CA) at 37°C in 5% CO_2.

Construction of expression plasmids

To obtain complete cDNA of mouse GPM6A, a reverse transcription (RT) polymerase chain reaction (PCR) was performed using mouse brain mRNA (Takara Bio Inc., Shiga, Japan). RT was carried out using random hexamers at 37°C for 60 min according to the manufacturer's instruction for First-Strand cDNA Synthesis Kit (Amersham Biosciences, Buckinghamshire, UK). cDNA fragments encoding mouse (nucleotides 438–1274) GPM6A were amplified using the primer set. PCR was carried out for 30 cycles. The reaction cycle was set at 95°C for 30 s, 60°C for 30 s, and 72°C for 30 s. The PCR-amplified fragment was cloned into pGEM-T Easy (Promega Corp., Madison, WI, USA), giving in pGEM–mM6A, and the inserted DNA was sequenced. The fragment of mouse GPM6A was ligated into pcDNA3.1 (+) vector (Invitrogen), generating pmM6A.

To express shRNA in ES cells, we constructed shRNA expression plasmid under the control of a U6 promoter against mouse and human GPM6A. Two DNA oligonucleotides (GPM6A; oligonucleotide A 5'-ACCGCAGATGTGTG AGCGCTTGGTTTCAAGAGAACCAAGCGCTCACACATC TGCTTTTTC-3' and oligonucleotide B 5'-TGCAGAAAAA GCAGATGTGTGAGCGCTTGGTTCTCTTGAAACCAAGC GCTCACACATCTG-3', Control; oligonucleotide C 5'-ACC GGGGGGGACCCCCCCTAAATTTTCAAGAGAAATTTA GGGGGGGTCCCCCCCTTTTTC-3' and oligonucleotide D 5'-TGCAGAAAAAGGGGGGGACCCCCCCTAAATTTCTC TTGAAAATTTAGGGGGGGTCCCCCC-3') were annealed and ligated into the siSTRIKE Neomycin vector (Promega) according to the manufacturer's instructions, resulting in psTN–mG6A1 and psTN–NSP1, respectively. All recombinant DNA experiments conformed to National Institute of Health (NIH) guidelines.

Stable expression of mouse GPM6A in COS-7 cells

COS-7 cells were transfected with the full-length mouse GPM6A cDNA in pmM6A by LipofectAMINE 2000 (Invitrogen), according to the manufacturer's instructions. In brief, 24 h after transfection, cells were treated with 200 μg/ml G418 (Invitrogen) for 2 weeks. G418-resistant colonies were identified, and independent colonies were reseeded in 10% DMEM, as described earlier. GPM6A expressing COS-7 cells (COS-mM6A) were identified using real-time PCR, as described.

Transfection with psTN–mG6A1 in mouse ES cells

For stable expression of shRNA against GPM6A in D3 cells, 8×10^6 cells were electroporated at 0.25 kV and 500 microfarads using 20 μg of psTN–mG6A1 or psTN–NSP1 (control). After replating, the cells were treated with 200 μg/ml G-418 for 1 week. G418-resistant colonies were identified using PCR, and independent colonies were reseeded in ES growth medium, as described earlier. The established cell lines were stained by antibodies against OCT3/4 (Santa Cruz Biotechnology Inc., Santa Cruz, CA, USA), Nanog (Santa Cruz), and SSEA-1 (Chemicon), respectively, as described subsequently. Transfected ES cells were differentiated into NSC and neuronal cells, as described subsequently.

Neural differentiation from mouse ES cells

Undifferentiated ES cells were differentiated into NSC and neuronal cells according to the method of Nakayama et al. [7]. Undifferentiated ES colonies were picked up and cultured in ACM (Sumitomo Bakelite Co. Ltd., Tokyo, Japan) under free-floating conditions for 6 days with undifferentiated mouse ES cells. NS spheres, which were induced colonies with undifferentiated mouse ES cells, were plated on poly-L-lysine (PLL) plus laminin (LAM)-coated plates (AGC Techno Glass Co., Ltd., Chiba, Japan) and differentiated with NS medium (NSM: NEUROBASAL medium (NBM) supplemented with B27 supplement, 2 mM L-glutamine, 20 ng/ml fibroblast growth factor-basic (bFGF; R&D Systems, Minneapolis, MN)), and recombinant human epidermal growth factor (EGF; R&D Systems) at 37°C in 5% CO_2 for 1 week. The NS colonies were picked up and transferred onto PLL/LAM-coated plates in NSM at 37°C in 5% CO_2 for

1 week. Finally, NSC were plated on PLL plus LAM-coated plates and differentiated with ACM at 37°C in 5% CO_2 for 1 to 2 weeks.

NSC were stained by antibodies against Nestin (Chemicon) and Musashi (Abcam plc., Cambridge, UK), respectively, as described subsequently.

Real-time PCR

Real-time PCR was performed using a SYBR Premix Ex Taq (Takara Bio) and a SmartCycler system (Cepheid, Sunnyvale, CA, USA). cDNA synthesis was carried out using the First-Strand cDNA Synthesis Kit, as described earlier, and real-time PCR was performed through 40 cycles. The reaction cycle was set at 95°C for 5 s and 60°C for 20 s. Relative expression levels were calculated using the $\Delta\Delta C_T$ method with normalization to glyceraldehyde-3-phosphate dehydrogenase transcription. Primers were purchased form Takara Bio.

Immunostaining

Cells were fixed with 4% paraformaldehyde for 20 min and permeabilized with 0.1% Triton X-100 for 5 min at room temperature. Nonspecific antibody staining was blocked by incubation with 10% bovine serum albumin in phosphate-buffered saline (PBS) for 30 min at room temperature. After preincubation, the cells were incubated with anti-beta III isoform of tubulin (Tubb3; Chemicon), anti-microtubule-associated protein 2 (MAP2: Chemicon), anti-doublecortin (DCX; Santa Cruz), anti-choline acetyltransferase (ChAT: Chemicon), anti-glutamate decarboxylases (GADs: Chemicon), anti-gamma aminobutyric acid (GABA: Chemicon), anti-tyrosine hydroxylase (TH: chemicon), and anti-serotonin (Chemicon) overnight at 4°C. After three washes with PBS, the cells were incubated with Cy3-labeled anti-mouse IgG (Amersham Biosciences), Cy3-labeled anti-rabbit IgG (KPL Inc., Gaithersburg, MD), or Cy3-labeled anti-goat IgG (Zymed Laboratories, South San Francisco, CA, USA). After three washes, the cells were double stained with DAPI (4',6-diamidino-2-phenylindole, dihydrochloride; Dojindo Laboratories, Kumamoto, Japan) for 5 min. For the neuronal cell proportion study, immunoreactive cells were counted for five randomly selected fields, each of which included 200–1000 cells of three independent cultures. The number of total cells was counted by the number of DAPI-staining nuclei.

Statistical analysis

Data were expressed as the mean ± SE. Statistical signification was determined by the unpaired Student's *t*-test. All results were derived from three independent experiments, at least.

Results

Expression of mouse GPM6A in NSC derived from mouse ES cells

In the mouse, GPM6A is known to be expressed in neurons [8,9]. However, it is unclear whether mouse GPM6A is expressed in undifferentiated ES cells and/or in NSC derived from ES cells. To clarify this point, we performed real-time PCR using a specific primer set for mouse GPM6A transcripts. Mouse GPM6A expression was detected in NSC derived from mouse ES cells but was barely observed in undifferentiated mouse ES cells (Fig. 1A).

Inhibition of GPM6A in GPM6A-expressing COS-7 cells

To inhibit the expression of mouse GPM6A mRNA, we constructed an shRNA-encoding sequence against mouse GPM6A expression vector (psTN–mG6A1) and established mouse GPM6A–expressing COS-7 cells, named COS-mM6A cells. We first examined whether the psTN–mG6A1 plasmid can induce specific RNA interference in COS-mM6A cells. As shown in Fig. 1B, expression level of mouse GPM6A transcripts was markedly decreased by expression of shRNA against GPM6A compared with untransfected COS-mM6A cells (control: 100% ± 13.1%; mG6A1: 1.43% ± 0.16%). On the other hand, GPM6A expression was unchanged in COS-mM6A cells (control: 100% ± 13%; NSP1: 104% ± 6.01%) transfected with the control plasmid (psTN–NSP1), which encodes a nonspecific sequence (Fig. 1B). These results indicated that psTN–mG6A1 plasmid sufficiently suppresses the expression of mouse GPM6A transcripts in vitro.

Production of stable transfected ES cell lines

To investigate the function of GPM6A, we generated stable transfected ES cell lines using psTN–mG6A1 and psTN–NSP1 plasmids and subjected them to G418 selection. In addition, to identify the founder ES cell lines, we performed PCR using a specific primer set for a shRNA expression region on the shRNA expression vector and genome DNA extracted from each founder ES cell line. PCR results showed that all selected mouse ES cell lines were inserted with the shRNA expression region into the genome DNA (data not shown). Hence, we established mouse ES cell lines, named D3m-shM6A1, shM6A2, and shM6A3 (transfected psTN–mG6A1 plasmid), and D3m-Mock1 and Mock2 (transfected psTN–NSP1) cells. To confirm the undifferentiated state of these cell lines, we performed immunocytochemistry for undifferentiated markers. As shown in Fig. 1C, established mouse ES cell lines (D3m-shM6A1 and D3m-Mock1 cells) expressed undifferentiated markers such as OCT3/4, Nanog, and SSEA1 (Fig. 1C). Other established mouse ES cell lines also expressed undifferentiated markers (data not shown). To examine the potential of established ES cell lines for differentiation, we transplanted all established ES cell lines into SCID mice to produce teratomas. All established ES cell lines formed teratomas, and histological examination revealed that these teratomas contained various tissues derived from all three embryonic germ layers, such as squamous, cartilage, and muscle (data not shown). These results indicated that all established ES cell lines retained their pluripotent states.

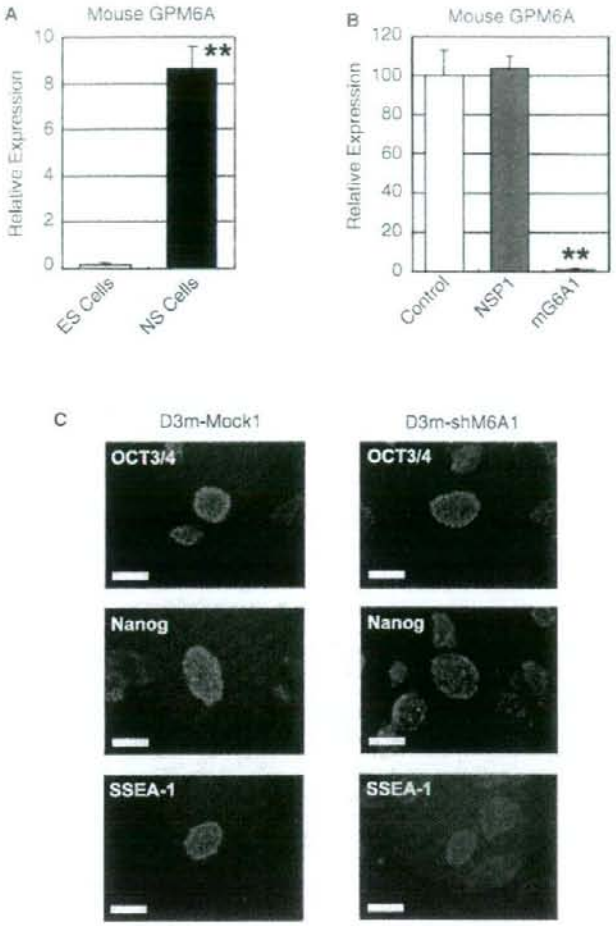

FIG. 1. Establishment of mouse embryonic stem (ES) cell lines expressing shRNA against mouse GPM6A transcripts. (**A**) Expression level of mouse GPM6A transcripts in undifferentiated mouse ES cells and neural stem cells derived from mouse ES cells. Total RNAs were extracted, and real-time PCR was performed using the SYBR Premix Ex Taq and SmartCycler systems. Values are expressed as the mean ± SE ($n = 4$). $^{**}p < 0.001$ compared with undifferentiated ES cells. (**B**) Suppression of mouse GPM6A transcript expression using shRNA vectors expressing shRNA against mouse GPM6A in COS-7 cells expressing mouse GPM6A. The psIN-mG6A1 or psIN-NSP1 plasmid was transiently expressed in COS-mM6A cells using LipofectAMINE 2000. Twenty-four hours after transfection, the total RNA was extracted from the transfected cells and real-time PCR was performed. Values are expressed as the mean ± SE ($n = 6$). $^{**}p < 0.001$ compared with control. NSP1 and mG6A1 indicate control and shRNA-expressing vector, respectively. (**C**) Detection of undifferentiated markers in undifferentiated D3m-Mock1 and D3m-shM6A1 cells. D3m-Mock1 and D3m-shM6A1 cells were positive for OCT3/4, Nanog, and SSEA-1. Scale bar = 50 μM. All experiments were independently carried out at least three times, and almost the same results were obtained each time.

Effect of GPM6A knockdown on neural differentiation

The undifferentiated ES cell colonies were picked up and cultured in ACM under free-floating conditions for 6 days, and the formed NS spheres were plated on PLL/LAM-coated plates in ACM for another 7 days. To investigate the effect of shRNA against GPM6A on neural differentiation, we performed real-time PCR with cDNAs from neural-differentiated D3m-Mock1 and D3m-shM6A1 cells. After 7 days' culture, the expression level of mouse GPM6A transcripts was suppressed in neural-differentiated D3m-shM6A1 cells (Fig. 2A: GPM6A: Mock1, 7.28 ± 2.39; shM6A, 1.57 ± 0.78). Under this condition, all examined neuroectodermal markers, i.e., OTX1, Lmx1b, En1, Pax2, Pax5, Sox1, Sox2, and Wnt1 were decreased in neural-differentiated D3m-shM6A1 cells compared with those of D3m-Mock1 cells (Fig. 2B). These results showed that suppression of mouse GPM6A transcripts decreased the expression levels of neuroectodermal markers in neural-differentiated D3m-shM6A1 cells. Next, we examined whether the expression levels of Tubb3 (immature neuron marker), MAP2 (mature neuron marker), DCX (migrating neuron marker), and Nestin (neuroepithelial marker) were decreased by the suppression of mouse GPM6A transcripts. The expression levels of Tubb3, MAP2, DCX, and Nestin transcripts were reduced in neural-differentiated D3m-shM6A1 cells (Fig. 2C) after 7 days' culture. To confirm whether the protein expression of Tubb3, MAP2, DCX, and Nestin decreased along with suppression of Tubb3, MAP2, DCX, and Nestin transcripts, we performed immunocytochemical analysis with antibodies against Tubb3, MAP2, DCX, and Nestin in neural-differentiated D3m-Mock1 and D3m-shM6A1 cells after 7 days' culture. As shown in Fig. 3, Tubb3, MAP2, DCX, and Nestin were detected in neural-differentiated D3m-Mock1 cells, but were

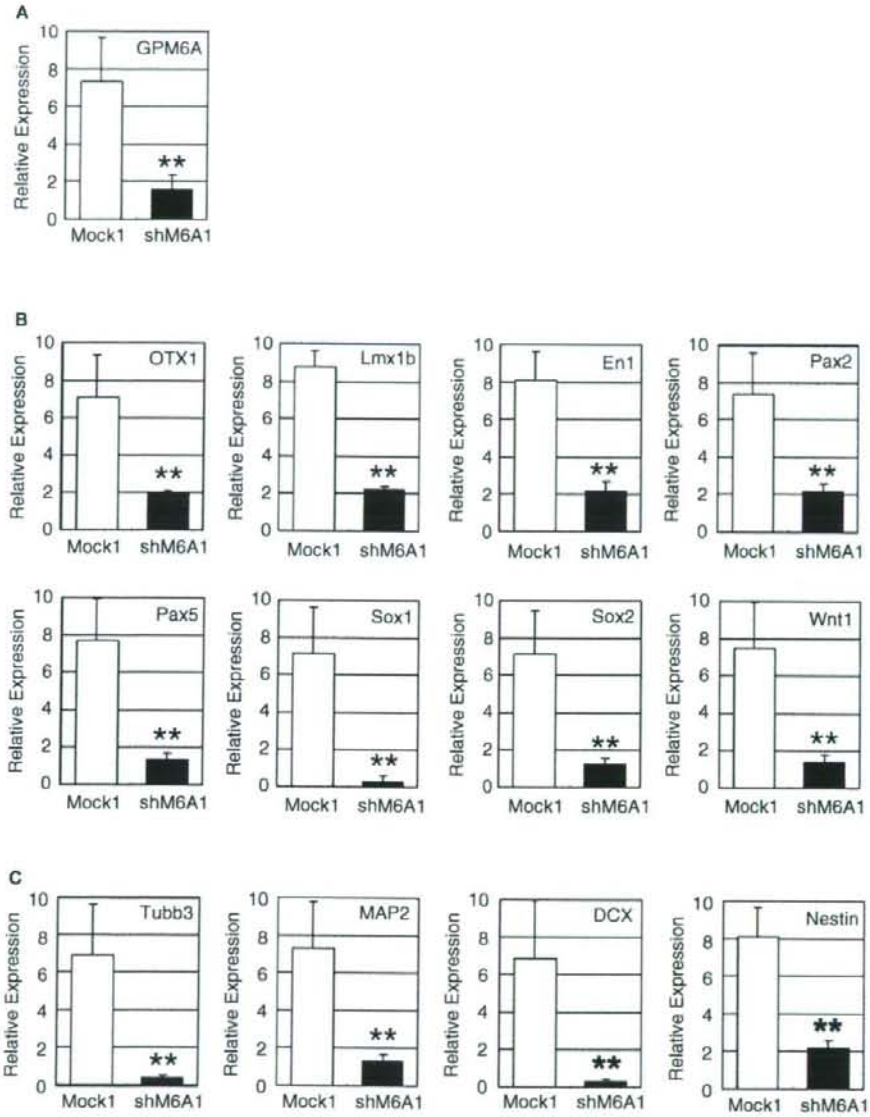

FIG. 2. Effect of shRNA against mouse GPM6A in neural differentiation. Real-time PCR was performed using specific primer sets and total RNAs from neural-differentiated D3m-Mock1 and D3m-shM6A1 cells. (**A**) Suppression of mouse GPM6A in neural-differentiated D3m-shM6A cells. (**B**) Expression levels of neuroectodermal markers in neural-differentiated D3m-Mock1 and D3m-shM6A1 cells. (**C**) Expression levels of mouse Tubb3, MAP2, DCX, and Nestin in neural-differentiated D3m-Mock1 and D3m-shM6A1 cells. One week after neural differentiation using astrocyte-conditioned medium (ACM), total RNA was extracted from the neural-differentiated cells and real-time PCR was performed. Values are expressed as the mean ± SE ($n = 8$). **$p < 0.001$ compared with neural-differentiated D3m-Mock1 cells. All experiments were independently carried out at least three times, and almost the same results were obtained each time.

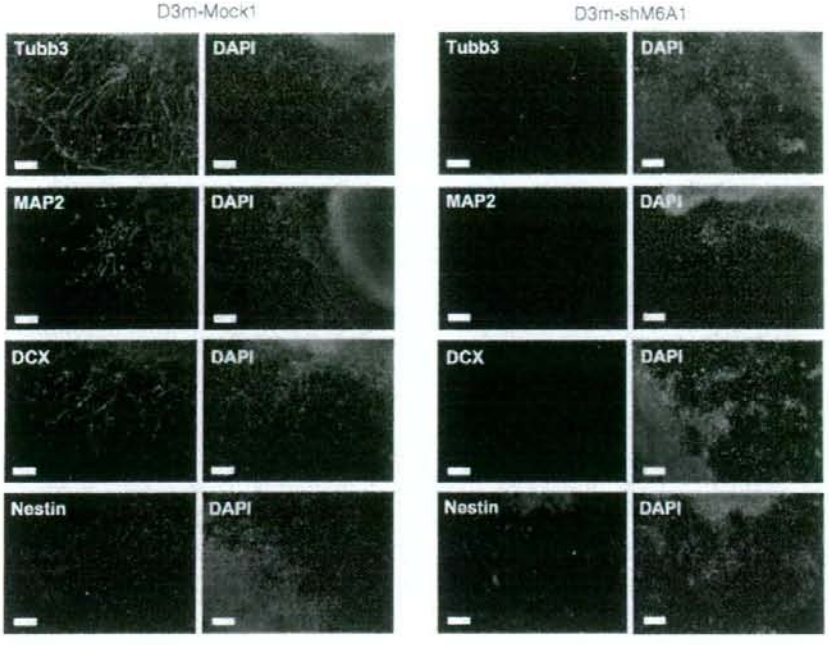

FIG. 3. Immunocytochemical analysis using anti-Tubb3, MAP2, DCX, and Nestin antibodies. Cells were differentiated with ACM for 1 week, fixed, and then immunostained with Tubb3, MAP2, DCX, and Nestin antibodies. DAPI was used for staining nuclei. Scale bar = 50 μm. All experiments were independently carried out at least three times, and almost the same results were obtained each time.

barely observed in neural-differentiated D3m-shM6A1 cells. The same results were obtained using D3m-shM6A2 and D3m-shM6A3 cells (data not shown). These results demonstrated that the suppression of mouse GPM6A transcripts using the shRNA expression vector caused a reduction of neuronal cell proportion. Therefore, it is suggested that mouse GPM6A is associated with the differentiation of neurons derived from undifferentiated mouse ES cells.

Decreased generation of NSCs derived from mouse ES cells expressing shRNA against GPM6A

As mentioned earlier, the suppression of mouse GPM6A expression reduced neuronal cell proportion derived from undifferentiated mouse ES cells. However, in neural differentiation, it is unclear whether GPM6A is involved in differentiation of undifferentiated ES cells to NSC and/or NSC to mature neurons. To evaluate the effect of shRNA against GPM6A on NSC generation, we performed neural differentiation and formed neurospheres using NSC from undifferentiated D3m-Mock1 and D3m-shM6A1 cells. Undifferentiated ES cell colonies were cultured in ACM under free-floating conditions for 6 days, and the formed NS spheres were plated on PLL/LAM-coated plates in NBM for another 7 days. After this period, we performed real-time PCR using the differentiated cells derived from undifferentiated D3m-Mock1 and D3m-shM6A1 cells. As shown in Fig. 4A, the expression levels of Nestin and Musashi transcripts, which are NSC markers [25,26], decreased in the differentiated cells derived from undifferentiated D3m-shM6A1 cells compared with those in undifferentiated D3m-Mock1 cells. Next, these differentiated cells (2.5×10^5 cells/ml), containing the NSC, derived from undifferentiated D3m-Mock1 and D3m-shM6A1 cells, were cultured in NBM under free-floating conditions for another 7 days. Under this culture condition, it is known that the NSC formed neurospheres [27,28]. The neurospheres formed from NSC derived from undifferentiated D3m-shM6A1 cells were clearly smaller in size and number compared with those formed from undifferentiated D3m-Mock1 cells (Fig. 4B and C; scale: D3m-Mock1 102 ± 19 μm, D3m-shM6A1 64 ± 21 μm; number: D3m-Mock1 864 ± 23 spheres/dish, D3m-shM6A1 298 ± 5 spheres/dish). To confirm whether the formed neurospheres were made of NSC, we performed immunocytochemical analysis using antibodies against Nestin and Musashi. Immunocytochemical analysis showed that neurospheres formed from NSC derived from undifferentiated D3m-Mock1 and D3m-shM6A1 cells were stained with antibodies against Nestin and Musashi, respectively (Fig. 4D). No significant differences in Nestin and Musashi dye patterns were apparent between the

neurospheres using NSC derived from undifferentiated D3m-Mock1 and those derived from undifferentiated D3m-shM6A1 cells. These results indicated that mouse GPM6A knockdown reduced, at least, differentiation proportion from undifferentiated mouse ES cells to NSC.

Reduction of neural differentiation proportion in mouse GPM6A knockdown

We showed earlier that mouse GPM6A knockdown decreased NSC generation derived from undifferentiated

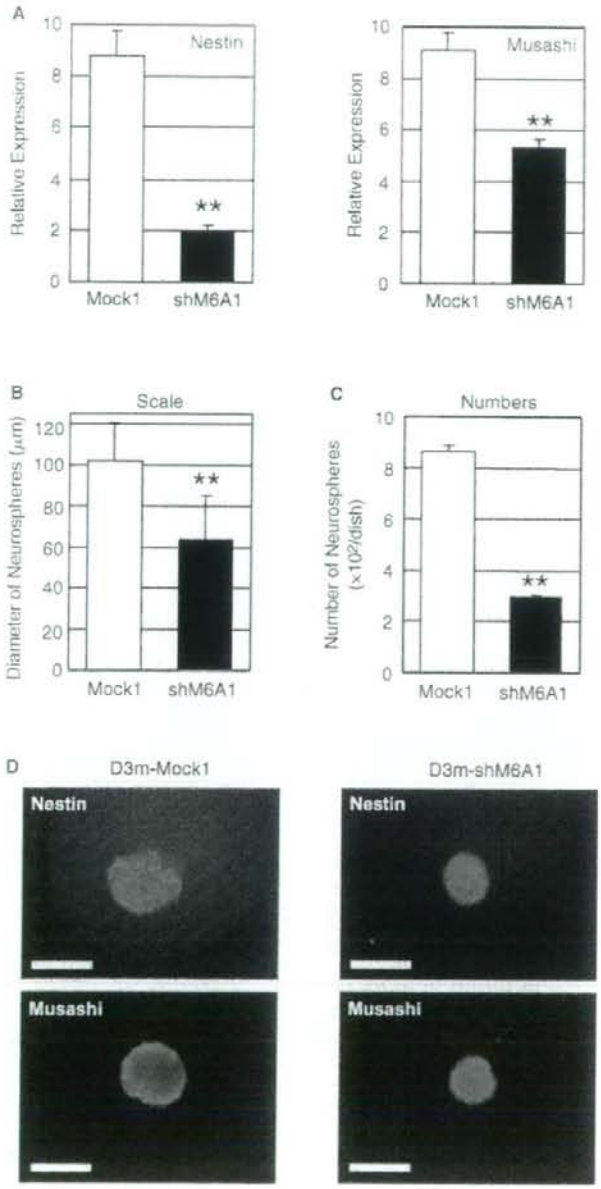

FIG. 4. Comparison of neural stem cells (NSCs) obtained from D3m-Mock1 and D3m-shM6A1 cells. (**A**) Suppression of Nestin and Musashi transcripts in neural-differentiated D3m-shM6A cells. Real-time PCR was performed using specific primer sets and total RNAs from neural-differentiated D3m-Mock1 and D3m-shM6A1 cells. Values are expressed as the mean ± SE (n = 8). $^{**}p < 0.001$ compared with neural differentiated D3m-Mock1 cells. (**B**) Scale of neurospheres derived from D3m-Mock1 and D3m-shM6A1 cells. (**C**) Number of neurospheres derived from D3m-Mock1 and D3m-shM6A1 cells. The differentiated cells (2.5×10^5 cells/ml) containing the NSC formed neurospheres in NBM supplemented with B27 after culture for 1 week. Values are expressed as the mean ± SE (n = 40). $^{**}p < 0.001$ compared with neurospheres from D3m-Mock1 cells. (**D**) Immunocytochemistry of neurospheres derived from D3m-Mock1 and D3m-shM6A1 cells. Neurospheres were fixed and immunostained with Nestin and Musashi antibodies, respectively. Scale bar = 100 μm. All experiments were independently carried out at least three times, and almost the same results were obtained each time.

mouse ES cells. To confirm whether the proportion of neural differentiation is decreased by GPM6A knockdown, we performed neural differentiation using NSC derived from undifferentiated D3m-Mock1 and D3m-shM6A1 cells. The neural differentiation was carried out using the same number of NSC derived from D3m-Mock1 and D3m-shM6A cells, respectively. NSC (2.5×10^5 cells/ml) derived from undifferentiated D3m-Mock1 and D3m-shM6A1 cells were plated on PLL/LAM-coated plates in ACM for 2 weeks. After 2 weeks' culture, the expression of mouse GPM6A transcripts was suppressed in neurons from NSC derived from D3m-shM6A1 cells (Fig. 5; GPM6A: Mock, 8.18 ± 1.78: shM6A, 1.89 ± 0.86). Expression levels of Tubb3, MAP2, and DCX were decreased in neurons from NSC derived from D3m-shM6A1 cells compared with those in D3m-Mock1 cells (Fig. 5). Further analysis indicated that ChAT, GAD1, GAD2, TH, and dopa decarboxylase (DCC) transcripts, all of which are neurotransmitter-related markers [29–31], were also decreased in neurons from NSC derived from D3m-shM6A1 cells compared with those in D3m-Mock1 cells (Fig. 5). These results indicated that expression levels of Tubb3, MAP2, DCX, ChAT, GAD1, GAD2, TH, and DCC transcripts were decreased by suppression of mouse GPM6A transcripts. Next, we performed immunocytochemical analysis with antibodies against neuronal and neurotransmitter-related markers, i.e. Tubb3, MAP2, DCX, ChAT, GADs, GABA, TH, and serotonin. Immunocytochemical analysis showed that Tubb3, MAP2, DCX, ChAT, GADs, GABA, TH, and serotonin-positive cells were decreased in neurons from NSC derived from D3m-shM6A1 cells after 2 weeks' culture (Fig. 6). Moreover, the percentage of Tubb3, MAP2, DCX, ChAT, GADs, GABA, TH, and serotonin-positive cells decreased in neural-differentiated cells derived from D3m-shM6A1 cells compared with those in D3m-Mock1 cells (Fig. 7). No discrepancy was found between the result of immunocytochemical analysis and that of real-time PCR. These findings indicated that mouse GPM6A knockdown also reduced the proportion of neuronal differentiation from NSC to neuronal cells.

Discussion

In mouse ES cells with suppressed expression of mouse GPM6A transcripts, we showed that the expression levels of NSC marker transcripts, which are Nestin and Musashi, decreased in differentiated cells derived from D3m-shM6A1 cells compared with those in D3m-Mock1 cells (Fig. 4A). The differentiated cells derived from D3m-Mock1 and D3m-shM6A1 cells were able to form neurospheres (Fig. 4B and C), and were immunoreactive for anti-Nestin and Musashi antibodies (Fig. 4D) [27,28]. However, neurospheres from D3m-shM6A1 cells are clearly smaller in size and number compared with those in D3m-Mock1 cells (Fig. 4A–C). These

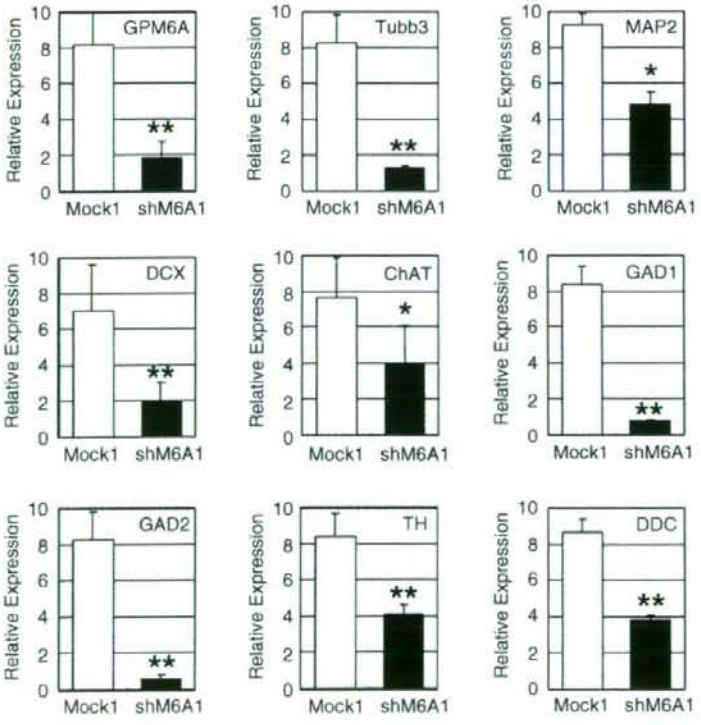

FIG. 5. Alterative expression level of neuronal markers between neural-differentiated D3m-Mock1 and D3m-shM6A1 cells. Two weeks after neural differentiation using ACM, total RNA was extracted from the neural-differentiated cells and real-time PCR was performed. Values are expressed as the mean ± SE ($n = 6$). *$p < 0.01$ and **$p < 0.001$ compared with neurons from D3m-Mock1 cells. All experiments were independently carried out at least three times, and almost the same results were obtained each time.

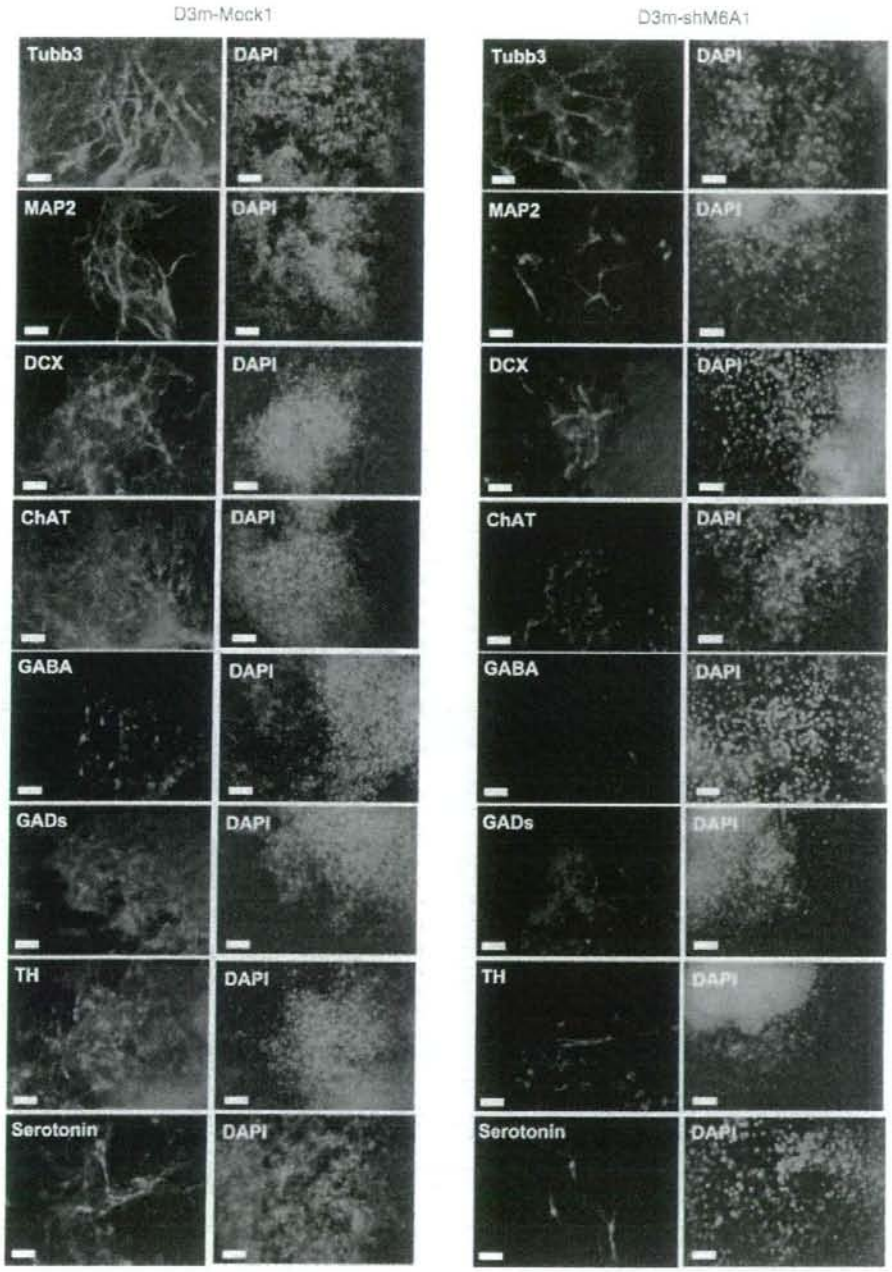

FIG. 6. Decrease of neural differentiation population in D3m-shM6A1 cells. Cells were differentiated with ACM for 2 weeks, fixed, and immunostained with Tubb3, MAP2, DCX, ChAT, GADs, GABA, TH, and serotonin antibodies. DAPI was used for staining nuclei. Scale bar = 25 μm. All experiments were independently carried out at least three times, and almost the same results were obtained each time.